Thermal behaviour and magnetic properties of Fe/Al_2O_3 multilayers

1994 J. Phys.: Condens. Matter 6 3337

(http://iopscience.iop.org/0953-8984/6/18/010)

J. Phys.: Condens. Matter 6 (1994) 3337–3346. Printed in the UK

Thermal behaviour and magnetic properties of Fe/Al_2O_3 multilayers

O Lenoble, Ph Bauer, J F Bobo, H Fischer, M F Ravet and M Piecuch
Laboratoire de Physique du Solide, Université de Nancy I, BP 239, 54506 Vandœuvre lès Nancy Cédex, France

Received 5 July 1993, in final form 11 January 1994

Abstract. We have deposited iron/alumina multilayers on sapphire wafers using RF magnetron sputtering. In the aim to study their thermal behaviour, multilayers have been annealed in a tubular furnace under a controlled atmosphere and characterized by x-ray diffraction, room-temperature bulk magnetization and ^{57}Fe Mössbauer spectroscopy. Without treatment, Fe/Al_2O_3 multilayers consist of alternating amorphous alumina and polycrystalline iron. For thermal treatments above 773 K, we observe the coexistence of Fe^{2+}, and metallic BCC and FCC Fe. The presence of these phases is related to the respective thicknesses of the Fe and Al_2O_3 layers for three different samples. Competition between the interfacial and shape magnetic anisotropy is found to be strongly dependent on the presence of FCC iron.

1. Introduction

The properties of metal–ceramic interfaces are of great interest in a large field of applications. From a metallurgical point of view, ceramic coatings are very efficient for the high-temperature protection of iron (used for instance in some matrices). In this case, one has to make sure that the coating of the matrix will have a good adhesion during many thermal cycles. This problem has been investigated by several groups [1, 2], but on a millimetre or micrometre scale (thick deposits or droplets). From another point of view, metal–oxide interfaces play an important role in electronic devices where conducting pathways are supported by an insulating layer [3]. Here, the stability of the device depends critically on the stability of the metal–ceramic bilayer. Finally, high-density storage media using the magneto-optic effect can include magnetic–dielectric multilayers. Magnetized layers induce the Kerr rotation of light, and dielectric layers contribute to increase this rotation via antireflective coupling. Here again, because of the laser recording procedure, the thermal stability of metal–ceramic interfaces plays an important role for the integrity of the medium. There are very few studies of such systems in the domain of multilayers, and so far researchers have studied only untreated samples [4].

All these facts have motivated us to study the physical properties of sputtered iron/alumina multilayers after several isochronal anneals. The structure and magnetism are investigated via x-ray diffraction, Mössbauer spectroscopy and bulk magnetization. We have already presented a study of low-temperature annealing (300–900 K) for this system [5]. Until now, we have mainly studied interdiffusion and the structural parameters of untreated multilayers. We try to report here data concerning the highest temperature where the artificial modulated structure is conserved and where the effect of such thermal treatments on the intrinsic structure of individual layers and on their magnetic properties is demonstrated.

0953-8984/94/183337+10$19.50

2. Experimental procedures

We use sapphire wafers as substrates; their preparation and the deposition of iron and alumina were carried out with an Alcatel SCM 650 automated sputtering apparatus using the RF magnetron process.

We have defined the following optimal preparation and growth conditions. First, a RF etch is performed on the substrate at 873 K for 30 min in an 8×10^{-3} mbar pure argon plasma. Then the deposition of iron and alumina is realized at room temperature by sequential exposure of substrates over the iron and alumina targets of 10 cm diameter. The distance between targets and substrate holder is fixed at 10 cm; the applied powers are 600 W and 300 W for iron and alumina, respectively. The determination of deposition rates has been done by small-angle x-ray scattering (SAXS) experiments on several single layers of iron or alumina with thicknesses ranging from 30 to 500 Å. The measurements of the positions of the Kiessig fringes give the thickness of the film. This leads respectively to 0.6 and 1.1 Å s^{-1}.

Samples are annealed in a tubular furnace under a 0.5 bar argon total pressure. They are introduced into the hot zone of the pre-heated furnace with a movable sample holder; the equilibrium temperature is then reached in less than 1 min. Samples are heated for 1 h at different temperatures ranging from 573 to 1373 K. They are checked by x-ray diffraction before and after anneal.

The microstructure of the multilayers considered is analysed with a combination of classical diffractometry in θ–2θ scan mode and grazing-incidence scattering (GIS). Diffractograms are recorded with the Co Kα filtered radiation on a θ–2θ Philips goniometer operating with a Raytech position-sensitive detector. It is well known that in the θ–2θ scan mode the detected diffraction comes only from crystallographic planes oriented parallel to the sample surface, while in GIS all the randomly distributed crystallites can be observed. The comparison of both kinds of scan indicates the potential layer texture. Moreover, in GIS the signal coming from a thin layer is favoured regarding the substrate; indeed, for the 3° incidence angle that we have chosen for phase growth observations, the optical path is enhanced and the penetration depth is of the order of 1000 Å. The interplanar distances deduced from diffraction peak positions are compared with the Joint Committee on Powder Diffraction Standards data for identifying the phases.

The artificial modulated superstructure is checked by SAXS. In the region spanning several degrees above the total reflection, the Bragg peaks resulting from the modulated superstructure can be observed. The average multilayer period Λ is deduced from their position using linear regression for the refraction correction. Experimental profiles are simulated by computed patterns using a recursive optical model [6] including the respective layer thicknesses and a period dispersion factor. The roughness of the interfaces is taken into account using the Debye–Waller factor:

$$r_{\mathrm{eff}} = r_{\mathrm{Fresnel}} \exp(-4\pi\sigma^2/\lambda^2)$$

where σ is the effective roughness.

Bulk magnetic measurements are performed, at room temperature, with a Micromag 2900 alternating-gradient magnetometer [7]. Hysteresis curves are recorded in either a parallel or a perpendicular configuration up to 15 kOe for complete saturation of the magnetization. Polar Kerr effect measurements are performed in the same conditions as below, at the He–Ne laser wavelength (633 nm).

Mössbauer spectra are recorded at room temperature in the back-scattering mode with a He–5% CH_4 gas flow proportional counter. This allows a non-destructive study with

a sampling depth of about 2500 Å, encompassing thus a number of Fe/Al_2O_3 bilayers ranging from 15 to 30 according to their nominal thickness. The source drive and data storage are of the usual design. The ^{57}Fe hyperfine pattern is fitted with standard routines where Lorentzian lineshapes are assumed. The characteristics of the samples devoted to this study are summarized in table 1. They have been designed to provide the best overview of the iron/alumina system; the thickness ratios $t_{Fe}/t_{Al_2O_3}$ vary from 1.4 to 0.17 while the individual layer thicknesses cover a large range (from 21 to 86 Å for Fe and from 61 to 150 Å for Al_2O_3). We have chosen samples with more than 20 bilayers in order to avoid spurious effects related to the substrate.

Table 1. Characteristics of our Fe/Al_2O_3 multilayers.

Sample	t_{Fe} (Å)	$t_{Al_2O_3}$ (Å)	Number of bilayers	Thermal annealing temperatures (K)
I	86	61	30	293, 973, 1073, 1373
II	21	65	50	293, 1073, 1273
III	25	150	100	293, 773, 1273, 1373

3. Results

3.1. X-ray diffraction

3.1.1. Untreated samples and low-temperature anneals. Before annealing, iron is BCC polycrystalline with a very small grain size and alumina is amorphous for all our samples. The fits of SAXS experiments lead to the same results for the series of as-deposited multilayers. The interface roughness is determined to be of the order of 1.5 Å, which means that interfaces are rather sharp, and the period dispersion, which is due to thickness disparities, is close to 4 Å. We only notice an increase in the iron grain size with increasing thickness of the iron layers on the one hand, and increasing annealing temperature for low-temperature thermal treatments (473–773 K) on the other hand. In this last case, growth is associated with a sharpening of the $Fe–Al_2O_3$ interface which we attribute to some segregation [5].

3.1.2. High-temperature anneals. For the higher-temperature anneals (present work), the x-ray diffraction results are presented in table 2. No data can be deduced for alumina from the x-ray spectra. For any samples and any thermal anneals we systematically observe α-Fe; it is a single phase up to 973 K and, above this temperature, it coexists with other phases such as $FeAl_2O_4$, FeAl and γ-Fe. The first finding is that γ-Fe appears only for samples II and III which have the largest $t_{Al_2O_3}/t_{Fe}$ thickness ratios. Furthermore, α-Fe is (110) textured for sample III annealed at 1273 K (figure 1). The integrity of the artificial structure has also been checked by SAXS as reported in table 2 and figure 2. We show here that the multilayer stack exists up to 1073 K for all samples.

Table 2. X-ray diffraction results for the series of samples.

	Phases present for the following temperatures				
Sample	293 K	973 K	1073 K	1273 K	1373 K
I	α-Fe[a]	α-Fe[a]	α-Fe	α-Fe	α-Fe
II	α-Fe[a]	α-Fe[a]	α-Fe[a]	α-Fe (110 textured)	α-Fe
			γ-Fe	γ-Fe	γ-Fe
III	α-Fe[a]	α-Fe[a]	Not studied[a]	α-Fe (110 textured)	α-Fe
				γ-Fe	$FeAl_2O_4$

[a] Artificial modulation still present.

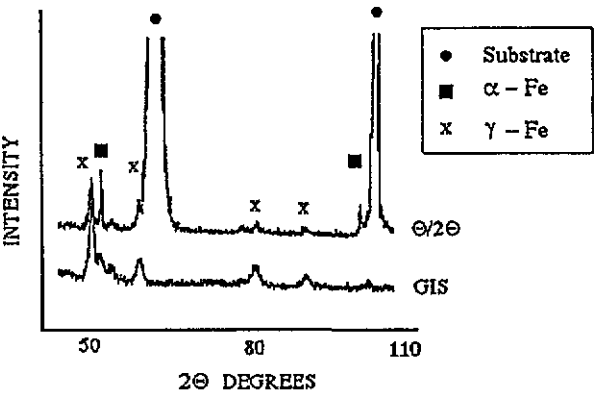

Figure 1. X-ray diffractograms for sample III annealed at 1273 K. The comparison between GIS and θ–2θ results indicates a (110) texture of iron.

3.2. Magnetization curves

Rough values of the magnetization of the three samples have been normalized to the standard effective magnetic field (electromagnetic units per cubic centimetre of iron). The experimental data are presented in figures 3(*a*), (*b*) and (*c*) for samples I, II and III, respectively. In-plane magnetization is favoured in all cases as all perpendicular magnetization curves are below the in-plane curves. These results allow us to estimate the average magnetization per iron atom and the magnetic anisotropy K_{eff} for each sample and each annealing temperature. The saturation moments per iron atom are reported in table 3. For untreated samples, saturation magnetizations are close to the bulk iron value (1707 G). The magnetic anisotropy K_{eff} has been evaluated for each sample. K_{eff} is the total area between the out-of-plane and the in-plane magnetization curves:

$$K_{\text{eff}} = \int_0^\infty (M_\perp - M_\parallel)\,\mathrm{d}H.$$

Several observations can be made from the anisotropy results. In the case of as-deposited samples, the evolution of $t_{\text{Fe}}K_{\text{eff}}$ from -9.8 erg cm^{-2} to -1.7 erg cm^{-2}, respectively, from sample III to sample I suggests that the stabilization of perpendicular anisotropy is possible for $t_{\text{Fe}} < 8$ Å. This thickness is lower than the minimum presented here (21 Å). Furthermore, anneals favour easier perpendicular magnetization; sample II at 1073 K and sample III at 1273 K are the most favourable for the stabilization of perpendicular magnetization. The presence of γ-Fe in both of these cases must be emphasized.

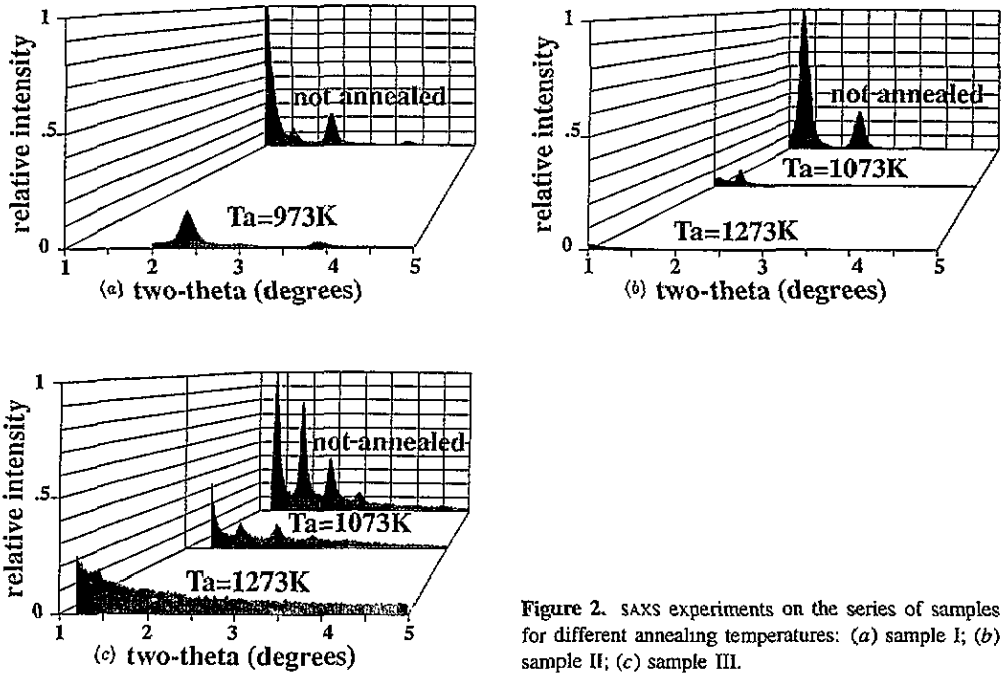

Figure 2. SAXS experiments on the series of samples for different annealing temperatures: (*a*) sample I; (*b*) sample II; (*c*) sample III.

Finally, Kerr loops confirm this effect of thermal treatments. It is accompanied by an increase in the absolute Kerr rotation (from 0.3° to 0.5° for sample II as deposited and annealed at 1073 K).

3.3. Mössbauer spectroscopy

Some experimental and calculated spectra are displayed in figures 4–6 representative of their evolution versus annealing temperature T_a and layer thickness. The spectral analysis is carried out mostly with one or two six-line patterns (magnetic phases) plus a quadrupole split doublet and a single line in the central part (non-magnetic phases). The magnetic components are attributed, respectively, to pure BCC iron and to iron atoms with aluminium in their neighbourhood, whereas the paramagnetic components are relevant, respectively, to an Fe^{2+} species according to its isomer shift, and to FCC iron (austenite). In fact, one observes strikingly different evolutions of the spectral shape from sample to sample with increasing annealing temperature.

The behaviour of sample I from the as-deposited state to the annealed state at 1373 K can be readily interpreted as follows. The spectra in figure 4 exhibit only two magnetically split subspectra. The hyperfine parameters of the major component correspond to undisturbed BCC iron whereas a decrease in the hyperfine field accompanied by an increase in the isomer shift is found for the minor subspectra. Prior to heating, this second component is actually a hyperfine field distribution related to iron atoms involved in an Fe–Al interface. The relative abundance computed from the spectrum in figure 4(*a*) suggests 7 Å of iron involved in an Fe–Al interface on each side of an iron layer. This interface is more extended than that deduced from SAXS data analysis since this last technique is less sensitive to local roughness. Moreover, the intermixing region in the iron layers presents a poor optical contrast inappropriate for SAXS.

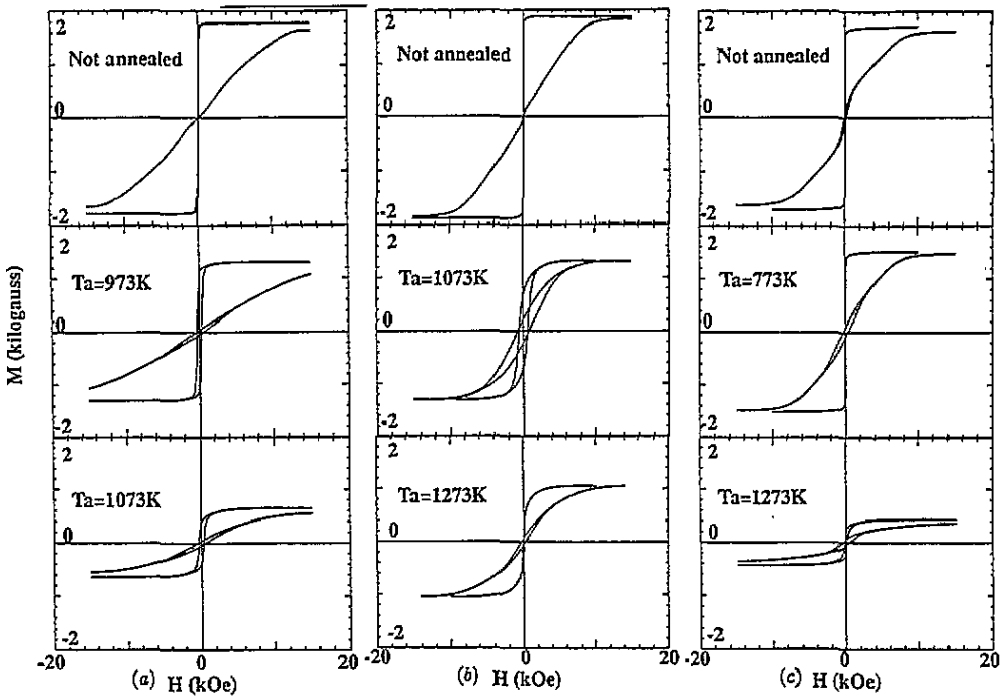

Figure 3. Magnetization curves normalized to electromagnetic units per cubic centimetre: (*a*) sample I; (*b*) sample II; (*c*) sample III.

Table 3. Saturation magnetization values M_s for the series of samples.

	M_s (μ_B/Fe atom) for the following temperatures			
Sample	293 K	973 K	1073 K	1273 K
I	2.26	1.67	0.83	
II	2.35		1.67	1.17
III	2.16			0.56

After annealing at 1373 K, no line broadening is found for the minor component and its hyperfine parameters are close to those of iron atoms having at least one aluminium atom as their first neighbour [8]. The spectral areas indicate the $Fe_{0.96}Al_{0.04}$ compound. Furthermore, the intensity ratio of the main magnetic component is 3:4:1,1:4:3 for the as-deposited sample, indicating that the magnetic moments lie almost in the film planes. After annealing, this ratio is 3:3.4:1,1:3.4:3, i.e. more of less representative of bulk magnetic anisotropy. These features confirm that the sample has evolved from a multilayered structure to an almost Fe–Al random solid solution during the annealing.

For samples II and III as-deposited with smaller iron thicknesses, the hyperfine fields of the magnetic components (related, respectively, to BCC iron and iron involved in the interfaces) are reduced by about 10 kOe when compared with sample I. Such a reduction in the hyperfine field must be connected to pressure effects [9], i.e. the as-deposited material is probably submitted to considerable internal stress. After annealing at 1073 K for sample II

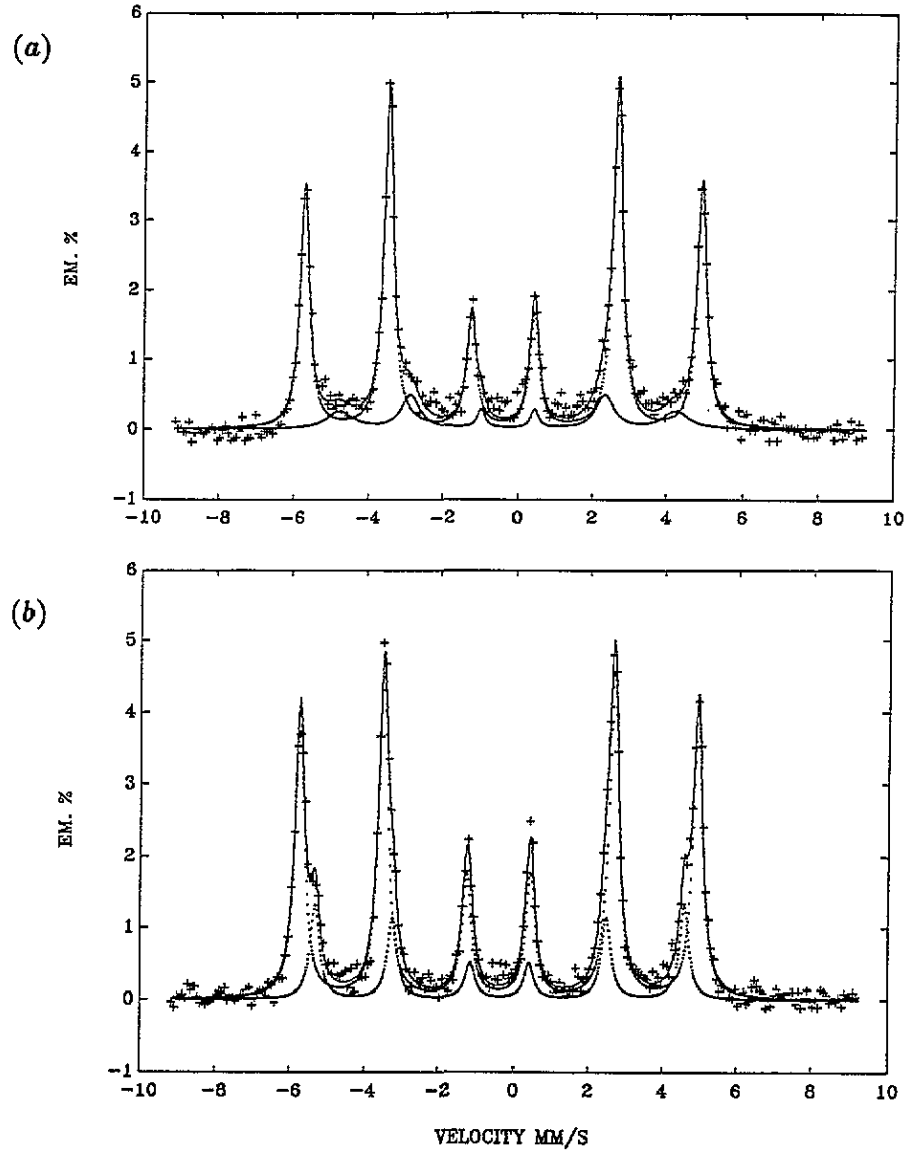

Figure 4. Mössbauer spectra for sample I: (*a*) untreated; (*b*) annealed for 1 h at 1373 K.

and at 1273 K for sample III, this stress vanishes at least in the α-phase, since the iron sextet recovers its normal hyperfine field.

Let us discuss separately for sample II and III the behaviours of the other subspectra versus the annealing temperature T_a (figures 5 and 6).

Starting with sample II, one observes the appearance of an austenite phase, the amount of which goes through a maximum of 32% at 1073 K (figure 5(*a*)). Although the isomer shift is the same as for stainless steel, the sharpness of the single emission line indicates the absence of foreign atoms in this FCC iron phase. Moreover, for $T_a = 1073$ K, no Fe–Al interface contribution is found, the sole magnetic component being standard BCC iron. After annealing at 1373 K, the magnetic part is made up of three sextets (figure 5(*b*)). The hyperfine

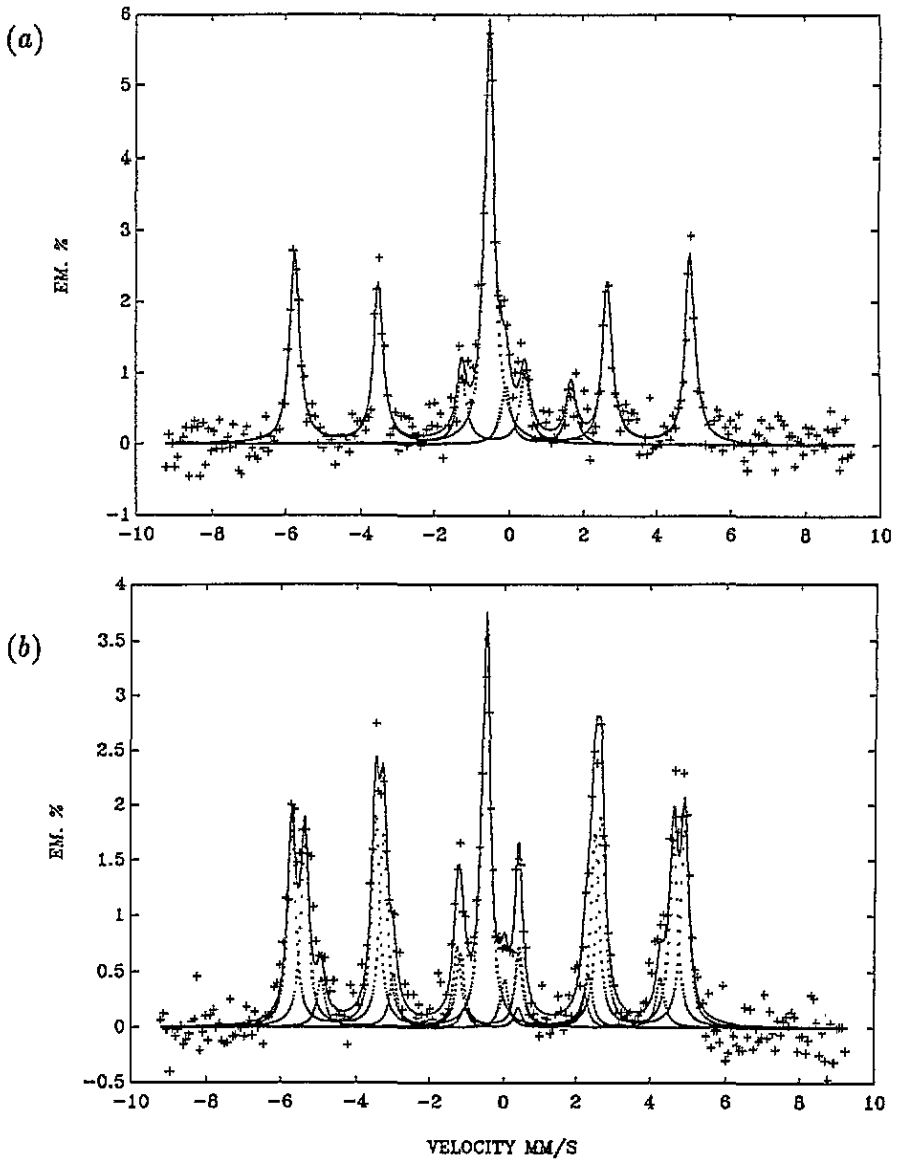

Figure 5. Mössbauer spectra for sample II: (*a*) annealed for 1 h at 1073 K; (*b*) annealed for 1 h at 1273 K.

parameters correspond, respectively, to iron without Al, iron with one Al atom and iron with two Al atoms as their first neighbours. The intensity behaviour, which follows a binomial law closely, is consistent with an almost homogeneous $Fe_{0.9}Al_{0.1}$ solid solution. Meanwhile, the magnetic anisotropy shows about the same trends versus T_a as encountered for sample I; the as-deposited structure exhibits dominant shape anisotropy (magnetic moments parallel to the layers) whereas for the alloy obtained after annealing at 1373 K the moments are nearly random in space. These conclusions point to the transformation of the initial multilayer stacking towards an Fe–Al solid solution for $T_a > 1073$ K but with a greater aluminium content than sample I. We also notice a decrease in the Fe^{2+} doublet abundance from 10%

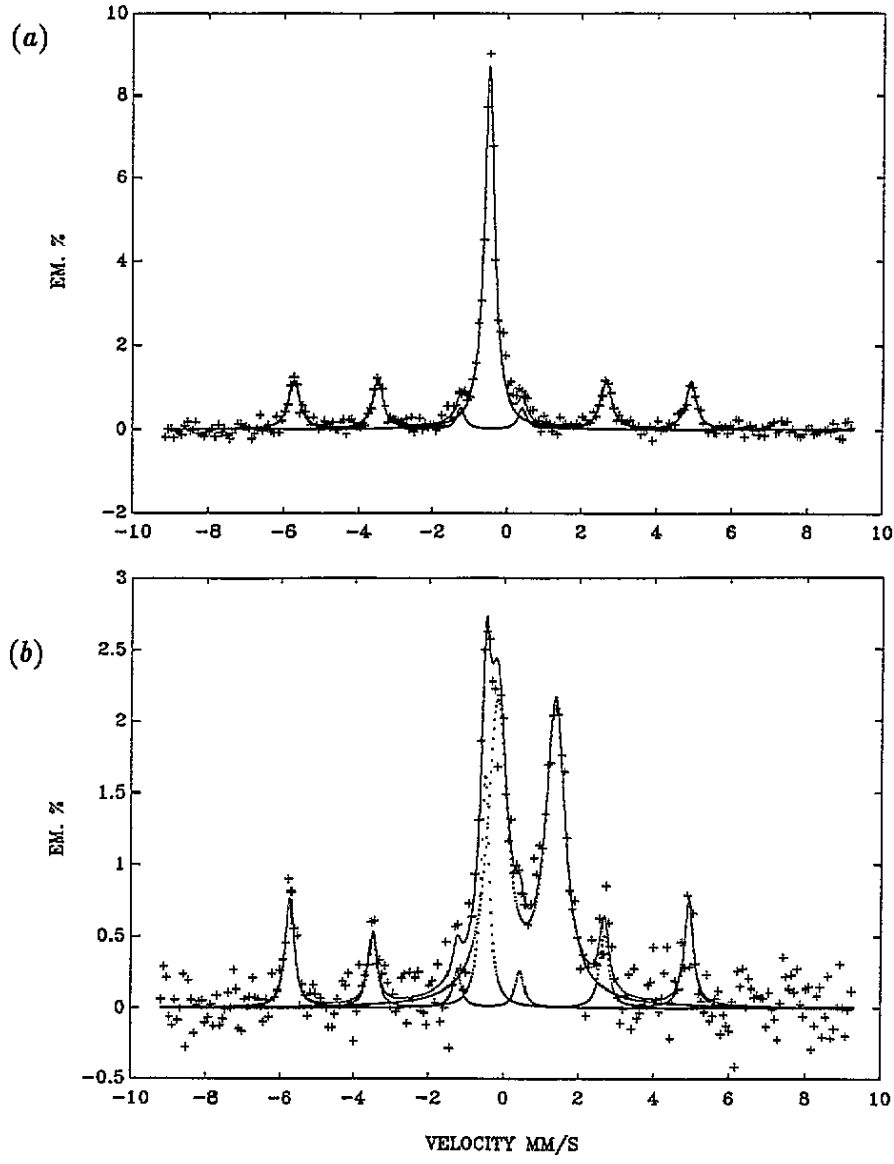

Figure 6. Mössbauer spectra for sample III: (*a*) annealed for 1 h at 1273 K; (*b*) annealed for 1 h at 1373 K.

(as-deposited) to 3% (T_a = 1373 K) and an increase in its quadrupole separation ΔE_q from 1.45 to 2.2 mm s^{-1} within the uncertainty due to poor spectral resolution.

For sample III, one observes about the same behaviour of the austenite amount variation but with an amazingly high value of 64% for T_a = 1273 K (figure 6(*a*)). The evolution of the magnetic anisotropy is similar to that of sample II with increasing T_a. In marked contrast, however, the Fe^{2+} species, which are almost absent in the spectra recorded for T_a up to 1273 K, represent 68% of the total emission area for T_a = 1373 K (figure 6(*b*)). Furthermore, no magnetic subspectrum related to any Fe–Al solid solution is to be found after the heat treatment. The quadrupole separation ΔE_q of the doublet (1.55 mm s^{-1}) is

comparable with that found for Fe^{2+} located at distorted tetrahedral sites of a partly inverted $FeAl_2O_4$ spinel [10, 11]. However, for the sample under consideration, this distortion is not likely to arise from an inversion since no Fe^{2+} species relevant to the octahedral B sites is evidenced here. Following [12], the ΔE_q separation of the latter would be 2.5 mm s^{-1}. This value is close to that found for Fe^{2+} in sample II for $T_a = 1273$ K; this might suggest a total inversion of the spinel structure for sample II after annealing.

4. Conclusion

We have prepared iron/alumina multilayers by RF magnetron sputtering on sapphire wafers. We have studied their structural and magnetic properties as a function of several thermal anneals.

Strikingly different evolutions, depending upon the respective iron thicknesses of the starting material, are observed through the thermal treatments. For sample I (thick iron layers), the stacking structure simply transforms to a random Fe–Al solid solution at high temperatures. In marked contrast, for samples with thinner iron layers (samples II and III), internal stress is found in the α-phase for the as-deposited state. When these samples are annealed, the disappearance of the stress in the α-phase is concomitant with the appearance of a γ-phase. At the same time, magnetic anisotropy deduced from magnetization measurements, as well as from ^{57}Fe Mössbauer spectroscopy, shows a tendency to perpendicular orientation of the moments. Even if we do not have any clear explanation for this, we think that the coexistence of the α- and γ-phases inside the iron layers might be responsible for this evolution. Anyway, we found this correlation between structural and magnetic properties to be an interesting result.

Moreover, for these two last samples, the disappearance of the multilayer structure at high temperatures leads to different final states with respect to the relative iron/alumina thicknesses; after the heat treatment, sample II (65 Å alumina) is made up of Fe–Al alloy with remaining γ-phase domains whereas sample III (150 Å alumina) consists of a spinel oxide with remaining relaxed α- and γ-iron domains.

In summary, our results emphasize the importance of parameters such as relative layer thicknesses and annealing temperatures upon the magnetic properties of the iron/alumina multilayers and the thermal evolution of the metal–ceramic interface.

References

[1] Klomp J T 1972 *Ceram. Bull.* **51** 683
[2] MacDonald J E and Eberhart J G 1965 *Trans. Metall. Soc. AIME* **233** 512
[3] Colaianni M L, Chen P J and Yates J T Jr 1990 *Surf. Sci.* **238** 13
[4] Senda M and Nagai Y 1989 *J. Appl. Phys.* **65** 3157
[5] Lenoble O, Bobo J-F, Piecuch M, Ravet M-F and Thomy A 1991 *Le Vide Les Couches Minces Suppl.* **258** 118
Lenoble O, Bobo J-F, Piecuch M and Ravet M-F to be published
[6] Piecuch M and Névot L 1990 *Mater. Sci. Forum* **59–60** 93
[7] Flanders P J 1988 *J. Appl. Phys.* **63** 3940
[8] Stearns M B 1972 *Phys. Rev.* B **6** 3326
[9] Pipkorn D N, Edge C K, Debrunner P, De Pasquali G, Drickamer H G and Frauenfelder H 1964 *Phys. Rev.* A **135** 1604
[10] Ono K, Ito A and Syono Y 1966 *Phys. Lett.* **19** 620
[11] Rossiter M J 1965 *J. Phys. Chem. Solids* **26** 775
[12] Yagnick C M and Mathur H B 1968 *J. Phys. C: Solid State Phys.* **1** 469